

---

# Tissue Detection In Ultrasound Images Using Real-Time Image Segmentation Model

---

**Zain M. Shariff**  
High School Student  
Curtis Junior High School  
University Place, WA 98467  
zainshariff6506@gmail.com

## Abstract

Medical ultrasounds visualize internal structures, like organs. A physician interpreting an ultrasound image must identify structure contours, brightness, and texture differences. YOLOv8 is a state of the art image segmentation model that indicates the contours of objects in an image. This study develops a real-time segmentation model that identifies tissue in ultrasound images. Ultrasound images were obtained, spliced into frames, and annotated in Roboflow. The Ultralytics library and Command Line Interface trained an image segmentation model. After 111 epochs of training, the model's performance increased. The 86th epoch produced the best model. It had a 0.85115 mAP50-95 rating and 0.91 F1 Score at 0.521 confidence. The model precisely identifies tissue in a 60 test image assessment. The model reliably predicted images in 300 ms or less. This study developed a model that can be utilized in real-time clinical practice. One application is automated demarcation of tissue with three dimensional modeling scans. Future studies integrating in-vivo organ structure ultrasound scans into the training dataset would develop a model competent for clinical practice.

## 1 Introduction

### 1.1 Ultrasounds

Ultrasounds are sound waves with frequencies higher than the upper audible limit of human hearing. Like audible sounds, ultrasounds bounce off of structures and provide information of the reflected structure. Ultrasounds are utilized in the medical field to visualize internal structures. As outlined in Ciccone and Grossman (2004), piezoelectric crystals in the ultrasound probe emit waves and receive information of the reflected waves. Reflected wave information includes distance traveled and the structure it reflected off of. The reflected waves are translated into an electrical signal which is represented in brightness on the display.

### 1.2 YOLOv8

Jocher et al. (2023) developed Ultralytics YOLOv8, a real time object detection and image segmentation model built on cutting edge advancements in deep learning and computer vision. YOLOv8 is suitable for a variety of applications and computer components. YOLOv8 offers instance segmentation, which goes beyond a simple bounding box image detection, able to display masks and contours that outline each object in an image. Recently, discussed in Semmler and Rose (2017) artificial intelligence is being increasingly used to help address tasks in a very efficient and accurate manner. This study strives to use YOLOv8 to automate the process of identifying tissue present in ultrasound scans to assist physicians in clinical care.

### 1.3 Goal

The goal of this study is to train and develop a machine learning model to reliably detect tissue in ultrasound scans. The output model must detect contours of tissue in ultrasound scans and output them in an orderly fashion. The model must reliably complete inferences in less than 400 milliseconds and be easily applicable in a variety of softwares and ultrasound scans. Additionally, the model should work with varying ultrasound scan types and point of views.

## 2 Materials and Methods

### 2.1 Materials

2 pieces of tissue (1 chicken muscular tissue and 1 lamb muscular tissue) were studied. A 3.5 MHz 2D Ultrasound was used to collect ultrasound images. A USB drive was used to transfer files from the Ultrasound Device to the computer system. For training, Ultralytics YOLOv8.1.0 was used through Command Line Interface. Roboflow was used to annotate the images.

### 2.2 Methods

A wet lab was set up, with a container filled with distilled water with experiment tissues were submerged in it. Ultrasound scans were obtained by placing a convex ultrasound probe about 2 cm away from the material. Ultrasound scans of 50fps in 3 seconds bursts, and 8 videos per piece of tissue were obtained. These scans were recorded on a USB drive and imported onto a computer. Videos were spliced into frames, 60 frames were set aside. Frames were imported into Roboflow for annotation. Manually, images were inspected for quality assurance. Tissue was segmented and annotated. Images were refitted to 800x600 px. Ultralytics was installed and annotated images were imported into the computer. A Command Line Interface command was issued to train a YOLO extra large segmentation model from scratch. At the end of the session, YOLO provided the best model from the whole session and a .csv file summarizing the training with pivotal data such as loss and metrics. The best model was obtained and assessed using the 60 image set. Assets are available at <https://github.com/zshar7/TissueDetection2024>.

## 3 Results

### 3.1 Overview

Lamb and chicken muscular tissue were analyzed in this study. A total of 1595 images were studied. It took 111 epochs to determine an optimal model. Predictions from the model can easily be executed through Command Line Interface. YOLO predictions were consistently finished in less than 300ms, and the best YOLO model was determined at the 86th epoch.

### 3.2 Training

Throughout training, YOLO outputted loss metrics of the best model in every epoch. YOLO measures four loss metrics: bounding box loss (Box Loss), segmentation loss (Seg Loss), classification loss (CLS loss), and Distribution Focal Loss (DFL). Box Loss and Seg Loss measures image area misidentified. CLS Loss determines overall incorrect predictions made by model. DFL works to help class imbalance and directly optimizes a distribution of bounding box borders. All across the board, when loss approaches zero, the model tends to be more accurate. As demonstrated in **Figure 1**, throughout training, the Box Loss, Seg Loss, CLS loss, and DFL decreased until a plateau and an increase at around the 100th epoch.

### 3.3 Post Training Assessment

#### 3.3.1 Precision and Recall

Precision and Recall are two principal and inverse metrics that one should study when training an artificial intelligence model. I strived for the developed model to have a balanced precision and recall.

The Precision Recall curve is shown in **Figure 2**. Performance metrics regarding precision and recall increased, shown in **Figure 1**.

### 3.3.2 mAP50 and mAP50-95

YOLO also outputs general performance metrics indicating model prediction improvement. Two overall metrics of success of the model are mAP50, and mAP50-95, which are further divided into Bounding Box type and Mask type. Bounding Box type deals with the circumscribed bounding box, and Mask type deals with the segmented prediction. mAP50 integrates the standard Precision-Recall curve and compares it with various classes and backgrounds, with a scale from 0 to 1. mAP50-95 also considers confidence thresholds, with a scale from 0 to 0.95. Overall as training continues, mAP50 and mAP50-95 values increased, showing an improvement in model prediction accuracy, shown in **Figure 1**. The best model found in the 86th epoch, had an mAP50-95 score of 0.85115.

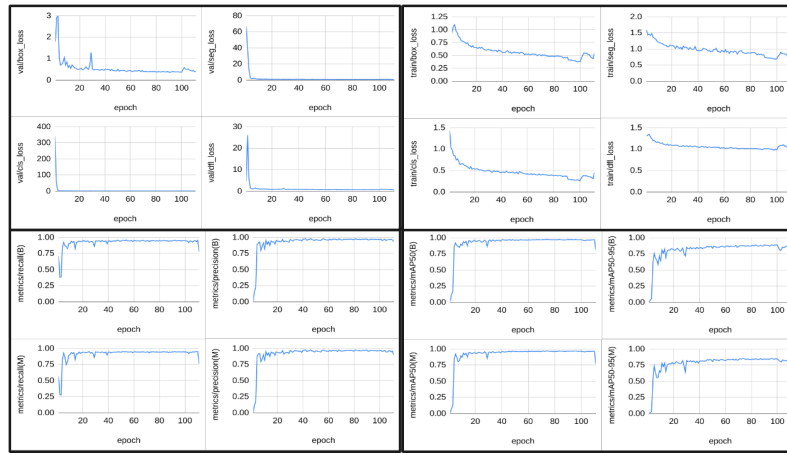


Figure 1: Training Data, Top Left: Validation Loss (best when approaches 0). Top Right: Training Loss (best when approaches 0). Bottom Left: Metric-based recall and precision (best when approaches 1). Bottom Right: mAP50 on Left (best when approaches 1) and mAP50-95 on Right (best when approaches 0.95).

### 3.3.3 F1 Confidence

Confidence thresholds are vital in developing image segmentation models. A confidence threshold determines how much confidence in an object results in confirmation or rejection. A high confidence means a high precision but a low recall. A low confidence means a low precision but a high recall. The F1 curve determines the optimal confidence threshold for a trained model. An F1 curve can help in indicating if precision and recall are balanced, if the F1 score is indicated with a confidence close to 0.5. The F1 score was 0.91 at 0.521 confidence.

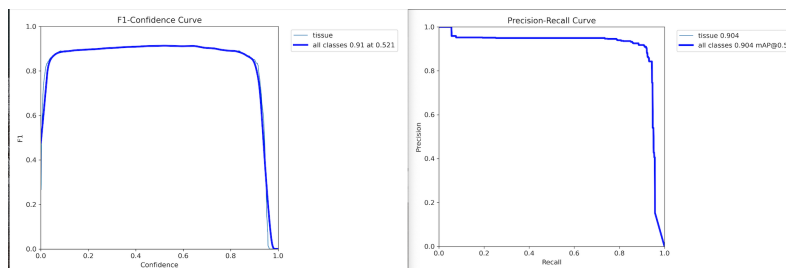


Figure 2: F1 Confidence Curve (left) and Precision Recall Curve (right)

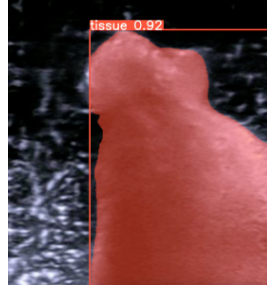


Figure 3: Example Prediction done by the best model

### 3.3.4 Test Images

The 60 image video manually evaluated the model's performance. The model successfully and precisely marked out tissue in the assessment (one prediction is shown in **Figure 3**). All these results satisfy the criteria set for an optimal model to trace contours and identify tissue in ultrasound scans with precise image segmentation.

## 4 Discussion

### 4.1 Other Related Research

Multiple two-dimensional slices at various imaging planes are obtained in the chamber of interest. The endocardial border from each image is traced either manually or using edge-detection software. Enriquez et al. (2018) demonstrated that mapping information can then be applied to this anatomic reconstruction. Ablations are critical in destroying abnormal electrical cells in the heart that can cause fatal issues such as tachycardia. A standard measurement or imaging technique to assist physicians in cardiac ablations does not exist. Shariff and Shariff (2024) found changes in ultrasound scans when exposing tissue to microwaves, especially the surface of the tissue. The superficial layers would reflect more ultrasounds with longer duration of exposure to microwaves. Shariff (2023) built on this and represented ultrasound scans in a polychromatic format for better appreciation of these patterns. In this study, a machine learning program with YOLOv8 was trained to run a segmentation algorithm on images. The best model obtained from the training can be used in real-time to display the contours of a detected tissue in ultrasound scans. The model is also saved and can be applicable in real world procedures regarding ultrasounds. Carneiro et al. (2012) developed a small-use deep learning model to perform segmentation on ultrasound scans of the left ventricle for possible three dimensional imaging and for diagnosis of certain conditions of patients. Hwang et al. (2015) created a neural network based artificial intelligence for classification of focal liver lesions using ultrasound scans.

### 4.2 Application of Study

The findings of this study, with additional research in clinical practice, can aid physicians performing ablations as a real-time assessment to determine the necessary amount of power and duration of ablation. As described in Capucci et al. (1997) most complications from atrial fibrillations (cardiac ablation procedure) are due to inadvertent lesions or excessive exposure harming normal functioning cells. The data from this paper should not apply to clinical practice. The report focuses on animal tissue, though similar, is not identical to abnormal electrical cells in the human heart. Abnormal electrical cells may possess different properties to animal tissue, normal cardiac electrical tissue, or even other abnormal electrical tissue. Furthermore, this is an ex-vivo study. During microwave ablation, tissue undergoes inflammation. These properties may have a significant impact on the model's accuracy to detect tissue. A relatively small size sample was investigated, a larger sample size may provide a reliable result with little chances of error. Further randomized evaluations are required to test the model's accuracy. Further studies are required to investigate if the findings of this study apply to clinical practice. Larger sample sizes are fundamental to support the reliability of the findings. The implementation of image machine learning models may be very useful to pinpointing the location of ablation lesions and extensively listing the state of the abnormal tissue.

## References

- Capucci, A., Villani, G. Q., and Aschieri, D. (1997). Risk of Complications of Atrial Fibrillation. *Pacing and Clinical Electrophysiology*, 20(10):2684–2691. \_eprint: <https://onlinelibrary.wiley.com/doi/pdf/10.1111/j.1540-8159.1997.tb06117.x>.
- Carneiro, G., Nascimento, J. C., and Freitas, A. (2012). The Segmentation of the Left Ventricle of the Heart From Ultrasound Data Using Deep Learning Architectures and Derivative-Based Search Methods. *IEEE Transactions on Image Processing*, 21(3):968–982. Conference Name: IEEE Transactions on Image Processing.
- Ciccone, T. J. and Grossman, S. A. (2004). Cardiac ultrasound. *Emergency Medicine Clinics*, 22(3):621–640. Publisher: Elsevier.
- Enriquez, A., Saenz, L. C., Rosso, R., Silvestry, F. E., Callans, D., Marchlinski, F. E., and Garcia, F. (2018). Use of Intracardiac Echocardiography in Interventional Cardiology. *Circulation*, 137(21):2278–2294. Publisher: American Heart Association.
- Hwang, Y. N., Lee, J. H., Kim, G. Y., Jiang, Y. Y., and Kim, S. M. (2015). Classification of focal liver lesions on ultrasound images by extracting hybrid textural features and using an artificial neural network. *Bio-Medical Materials and Engineering*, 26(s1):S1599–S1611. Publisher: IOS Press.
- Jocher, G., Chaurasia, A., and Qiu, J. (2023). Ultralytics YOLO. original-date: 2022-09-11T16:39:45Z.
- Semmler, S. and Rose, Z. (2017). Artificial Intelligence: Application Today and Implications Tomorrow. *Duke Law & Technology Review*, 16:85.
- Shariff, Z. (2023). Microwave-Related Tissue Changes Using Ultrasound: Processing Images into Spectral Colors.
- Shariff, Z. and Shariff, N. (2024). Identification of microwave-related changes in tissue using an ultrasound scan. *Journal of Emerging Investigators*.